Biomolecular Assembly

DOI: 10.1002/ange.201303854

Controlled Alignment of Filamentous Supramolecular Assemblies of Biomolecules into Centimeter-Scale Highly Ordered Patterns by Using Nature-Inspired Magnetic Guidance**

*Binrui Cao, Ye Zhu, Lin Wang, and Chuanbin Mao**

Filamentous supramolecular assemblies of biomolecules, such as bacterial flagella,[1] bacterial pili,[2] and bacteriophages (also called phages),[3] are naturally occurring nanofibers assembled from their subunits in a highly ordered fashion. Owing to the structural ordering, chemical and thermal stability, and genetically tunable surface chemistry, biological nanofibers can be used as templates for directing the synthesis and assembly of functional nanomaterials such as bone minerals[4] and silica.[5] However, to assemble biological nanofibers into controlled structures at a large scale (e.g., up to centimeter scale) is still a challenge. Currently, several methods have been tried to form assemblies of biological nanofibers, including electrostatic interactions,[4a] liquid-crystalline assemblies,[6] capillary forces,[7] and molecular recognitions.[2a] However, these methods are relatively complicated in handling and most of them (except the liquid-crystalline assembly method) can only generate small-scale nanostructures. Furthermore, although large-scale vertical assemblies of filamentous inorganic hard nanostructures such as nanotubes of boron carbonitride,[8] carbon,[9] as well as titania,[10] and nanowires of GaAs,[11] Si,[12] ZnO,[13] and cadmium chalcogenide,[14] have been reported, to our knowledge, no method for the large-scale vertical assembly of filamentous soft biological nanofibers has been reported to date. To advance the practical use of biological nanofibers with various shapes and functionalities in building devices, it is important to have a facile method that can lead to either single- or multilayered assemblies with controlled (either horizontal or vertical) orientation of constituent biological nanofibers on a solid substrate. Therefore, a method that is easy to handle is needed to assemble the biological nanofibers into large-scale assemblies with controlled orientation.

In nature, Fe_3O_4 is present in many organisms such as magnetotactic bacteria (MTB), honey bees, pigeons, dolphins, and butterflies,[15] allowing the magnetic dipolar field of the earth to assist their orientation, navigation, or homing. MTB, as one of the most well-known examples, are capable of taking up Fe sources and converting them into magnetic nanoparticles (MNPs) such as Fe_3O_4 or Fe_3S_4 in vivo.[16] As a result, MTB become oriented along the magnetic field lines of the magnetic field of the earth simply because they contain MNPs.[16] The magnetically guided orientation of organisms such as MTB simply because of their association with MNPs inspired us to use a magnetic field to guide the assembly of biological nanofibers with the help of MNPs (Figure 1a). Although the arrangement of synthetic MNPs along magnetic lines was applied to align MNPs themselves,[17] carbon nanotubes,[18] and polymers,[19] using them to guide the alignment of biological nanofibers into long-range-ordered patterns has not been reported to date. Here, we report the controlled alignment of three structurally different types of biological nanofibers, including wave-like bacterial flagellar filaments (termed flagella for convenience), straight type 1 bacterial pili, and the semiflexible M13 phage. These nanofibers were first decorated with Fe_3O_4 MNPs into long-range-ordered arrays by simply varying the direction and strength of the external magnetic field. Single-orientation arrays (Figure 1b), where biological nanofibers were parallel to each other, were fabricated by applying a magnetic field with its direction parallel to the substrates. Multi-orientation multilayered assemblies of biological nanofibers were synthesized through layer-by-layer deposition with the magnetic field alternatively twisted for each alternating layer. During the formation of such assemblies, biological nanofibers were aligned parallely into one single-orientation layer along one magnetic field and then the magnetic field was twisted into another direction to align the nanofibers into a neighboring single-orientation layer (Figure 1c). In the multi-orientation multilayered assemblies, the orientation of nanofibers in each layer was parallel to the external magnetic field (Figure 1c). When the magnetic field was twisted during the deposition of biological nanofibers, a new neighboring layer made of nanofibers parallely aligned along a different orientation was formed. Vertically aligned nanofiber arrays (Figure 1d) could also be made by simply changing the external magnetic field to be perpendicular to the substrates. The degrees of ordering of the formed nanofiber arrays were also found to be affected by the strength of external magnetic fields (Figure S1 in the Supporting Information).

[*] B. R. Cao,[+] Y. Zhu,[+] L. Wang, Prof. C. B. Mao
Department of Chemistry & Biochemistry
Stephenson Life Sciences Research Center
University of Oklahoma
101 Stephenson Parkway, Norman, OK 73019 (USA)
E-mail: cbmao@ou.edu
Homepage: http://chem.ou.edu/chuanbin-mao

[+] These authors contributed equally to this work.

[**] This work was in part supported by National Science Foundation (DMR-0847758, CBET-0854414, CBET-0854465 and CMMI-1234957). For financial support we also thank the National Institutes of Health (R03AR056848, R21EB015190, R01HL092526), Department of Defense Peer Reviewed Medical Research Program (W81XWH-12-1-0384), Oklahoma Center for the Advancement of Science and Technology (HR11-006) and Oklahoma Center for Adult Stem Cell Research (434003).

Supporting information for this article is available on the WWW under http://dx.doi.org/10.1002/anie.201303854.

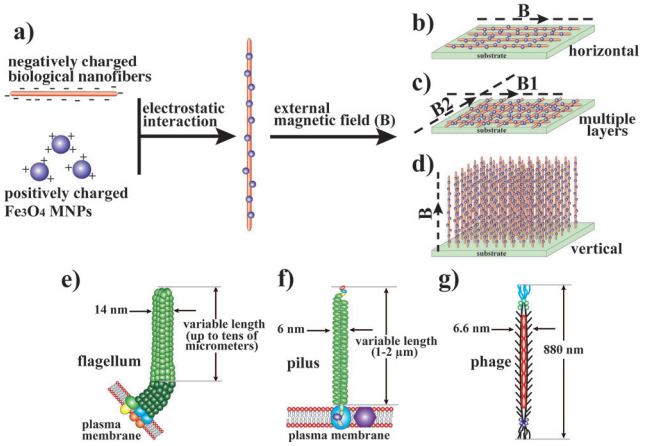

Figure 1. Illustration of using a magnetic field to guide the alignment of filamentous supramolecular assemblies of biomolecules with the help of magnetic nanoparticles. a) General idea of the method. Positively charged Fe_3O_4 MNPs interact with negatively charged biological nanofibers to form MNP–nanofiber complexes, which can be further guided by magnetic fields. b) Arrays of biological nanofibers aligned parallely with a single orientation. c) Multilayered assemblies of nanofibers with multiple orientations ("multi-orientation") formed by twisting the direction of the magnetic field for each neighboring layer. After one parallely aligned nanofiber layer is formed under the guidance of one magnetic field (B1), another layer of parallely aligned nanofibers is deposited under the guidance of a magnetic field with a different direction (B2). d) Vertically aligned nanofiber arrays guided by a magnetic field perpendicular to a substrate. e–g) Structures of three types of bacteria-related biological nanofibers: bacterial flagellum (e), which protrudes from the bacterial cell surface for assisting cell swimming, type 1 pilus (f), which is attached to the bacterial cell surface for assisting cell adhesion, and M13 phage (g), which is a virus specifically infecting bacteria.

It is known that most proteins and protein-based supramolecular assemblies are negatively charged with an isoelectric point (pI) below 7,[20] including the three filamentous supramolecular assemblies of biomolecules studied in this work, namely, bacterial flagellum (Figure 1e), type 1 bacterial pilus (Figure 1f), and M13 phage (Figure 1g). Flagellar filament is a wave-like nanofilament (14 nm wide and length tunable depending on the number of protein subunits) assembled from several thousand copies of protein subunits called flagellin (Figure S2a). The solvent-exposed domain of wild-type flagellin (FliC gene product) for bacteria contains negatively charged amino acids such as aspartic acid (D) and glutamic acid (E) with a pI estimated to be approximately 5.3.[21] Type 1 bacterial pilus is a rigid hair-like appendage (6 nm wide and 1–2 μm long; Figure S2c) found on the surface of bacteria. It is predominantly assembled from the protein subunit, FimA, and has a pI of approximately 3.9 at room temperature.[2] M13 phage (ca. 6.6 nm wide and 880 nm long), a semiflexible biological nanofiber (Figure S2d), is composed of circular single-stranded DNA (ssDNA) encapsulated in approximately 2700 copies of its major coat protein and capped with a few copies of minor coat proteins at both tips. The high copy numbers of solvent-exposed negatively charged amino acids in the N terminus of major coat proteins make M13 phage negatively charged with a pI of approximately 4.2.[3,5,20] Since most biological nanofibers are negatively charged, positively charged Fe_3O_4 MNPs were used to electrostatically interact with them to achieve the assembly (and the consequent decoration) of MNPs along them, forming MNP–nanofiber complexes for alignment guided by a magnetic field. If the surface of a biological nanofiber changes to be positively charged owing to genetic engineering,[5] negatively charged Fe_3O_4 MNPs can also be synthesized to decorate the nanofiber for the alignment. Herein, we used negatively charged bacterial flagellum, type 1 bacterial pilus, and M13 phage as the examples for the study of the alignment of MNP-decorated biological nanofibers by external magnetic fields. The flagellum, pilus, and phage nanofibers were biologically produced and amplified following our reported procedures.[2a,21,22]

Positively charged Fe_3O_4 MNPs were synthesized following a reported method.[23] Briefly, a mixed solution of $FeCl_2$ (4 mL, 1 M) and $FeCl_3$ (1 mL, 2 M, in 2 M HCl) was added to an ammonia solution (50 mL, 0.7 M). The black precipitates were collected by centrifugation (10 min at 7500 g), washed with nitric acid (2 M) and resuspended in water to form a transparent and uniform Fe_3O_4 MNP solution. The synthesized MNPs were analyzed by using the electron diffraction pattern (Figure S3a, inset)[24] and their diameter was 5–8 nm (Figure 2a). The measured room temperature hysteresis curves (Figure S3 b,c) show that the saturation magnetization and coercivity value of the as-synthesized MNPs are 35 emu g^{-1} and 8 Oe, respectively. When Fe_3O_4 nanoparticle solution was placed close to a magnet, Fe_3O_4 nanoparticles were attracted by the magnet (Figure 2a inset), which also confirmed the superparamagnetism of the synthesized Fe_3O_4 nanoparticles. The as-synthesized MNP solution (70 mg mL^{-1}, pH 4.0) was used directly in this work.

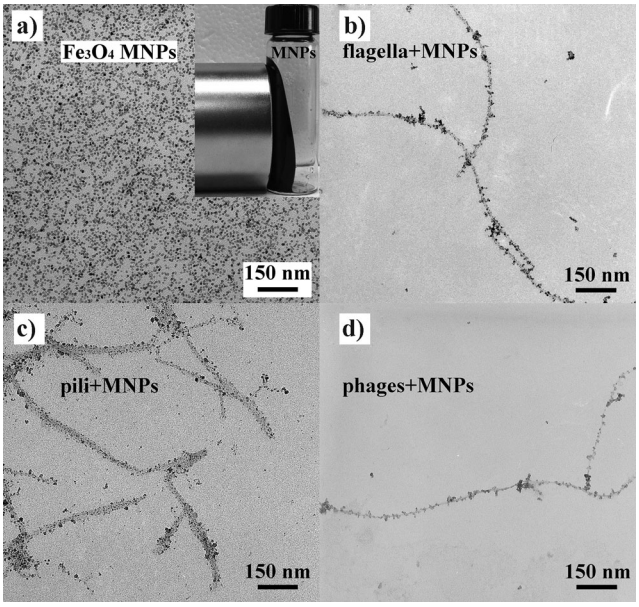

Figure 2. TEM images of Fe_3O_4 MNPs and MNP–nanofiber complexes formed by the assembly of MNPs along different biological nanofibers. a) As-synthesized Fe_3O_4 MNPs. Inset: the synthesized Fe_3O_4 MNPs can be attracted by a magnet. b) MNP–flagellum complexes. c) MNP–pilus complexes. d) MNP–phage complexes. In (b–d), the nanoparticles are coated on the surface of the biological nanofibers.

To verify the interaction between positively charged Fe_3O_4 MNPs and negatively charged biological nanofibers, they were mixed in an aqueous solution. Immediately, some rust-red precipitates were formed (Figure S4) owing to the coating of MNPs onto the biological nanofiber templates. Then the rust-red precipitates were observed by using a transmission electron microscope (TEM) and were found to be made of MNP–nanofiber complexes (Figure 2b–d), in which Fe_3O_4 MNPs were assembled along biological nanofibers (flagella, pili, or phages) to form a "beads-on-rods" structure. This fact indicates that our synthesized positively charged Fe_3O_4 MNPs can interact with negatively charged biological nanofibers through electrostatic forces to form MNP-decorated biological nanofibers.

To achieve single-orientation horizontally aligned nanofiber arrays (Figure 1b), Fe_3O_4 MNPs solution (70 mg mL^{-1}, pH 4) was mixed with nanofiber solution (flagellum solution, $OD_{280nm} = 0.1$; pilus solution, $OD_{280nm} = 0.25$; phage solution, 10^{13} pfu mL^{-1}; pfu: plaque forming unit; all biological nanofibers dissolved in water with pH 7.0) at a volume ratio of 1:49 (MNP/biological nanofiber) to form MNP–nanofiber complexes, respectively, and then air-dried on a cover slide in a constant magnetic field (1 T) with a direction parallel to the surface of the cover slide (Figure 1b). The size of assembled MNP–nanofiber structures could reach up to centimeter scale (Figure S5). The scanning electron microscopy (SEM) and optical microscopy results (Figure 3) showed that not only Fe_3O_4 MNPs (Figure 3a) but also MNP–nanofiber complexes (flagellum: Figure 3b and Figure S6a; pilus: Figure 3c and Figure S6c; phage: Figure 3d and Figure S6e) could be parallely aligned along the direction of the magnetic field perfectly. However, when not decorated with Fe_3O_4 MNPs, biological nanofibers were randomly oriented and not assembled into any aligned pattern even in the presence of a magnetic field (Figure S7). This fact confirmed that the alignment of the nanofibers was due to the alignment of their associated Fe_3O_4 MNPs guided by the magnetic fields. Notably, some biological nanofibers are flexible and curved in their natural form,[4a,21a,22] such as flagella (Figure 2b, Figures S2b and S8) and phages (Figure 2d, Figure S2c). But when they were decorated with MNPs and placed in magnetic fields, they became straight (Figure 3), thereby indicating the straightening of biological nanofibers is due to the alignment of associated Fe_3O_4 MNPs by magnetic fields. In addition, we used the flagellum–MNP system to systematically study the factors that may affect the biological nanofiber assembly, including the strength of the magnetic field, surface charge of the nanofibers, concentration of nanofibers and MNPs, and drying speed. These studies show that both the strength of the magnetic field (Figure S1) and the flagellum surface charges (Figure S9) greatly affect the ordering of the nanofiber arrays. Only when a relatively strong magnetic field (1 T; Figure S1a) is applied and flagella are used that have an overall surface charge opposite to that of the MNPs (i.e., slightly negatively charged WT flagella or more negatively charged flagella displaying peptide EEEEEEEE; Figure S9a,b), highly ordered arrays are obtained. The effects of concentrations of biological nanofibers (Figures S10 and S11) and MNPs (Figures S12 and S13) are trivial once the optical density at 280 nm (OD_{280nm}) of flagella and the mass concentration of MNPs are above 0.01 and 0.14 mg mL^{-1}, respectively. In addition, the drying speed, either fast drying in a flow of N_2 or slow drying in air (Figure S14), does not show any effect on the biological nanofiber assembly.

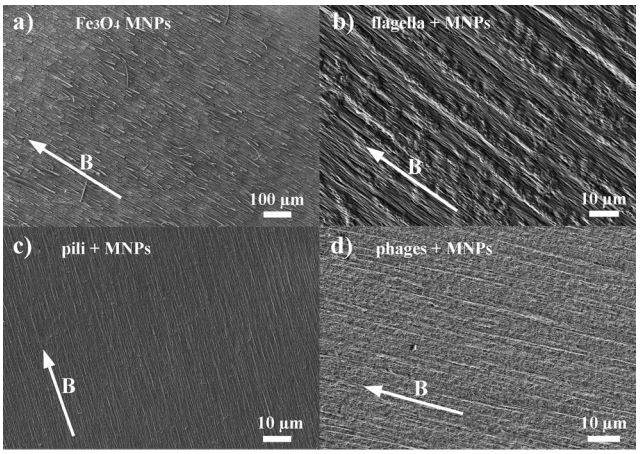

Figure 3. SEM images of the single-orientation horizontally aligned Fe_3O_4 MNPs and MNP–nanofiber complexes in the presence of magnetic fields (B, indicated by arrows). a) Aligned Fe_3O_4 MNPs. b) Aligned MNP–flagellum complexes. c) Aligned MNP–pilus complexes. d) Aligned MNP–phage complexes. The corresponding optical images of MNP–nanofiber complexes in the presence of magnetic fields can be found in the Supporting Information (Figure S6).

When the direction of the magnetic field was twisted every time after the deposition of a single-orientation layer under the guidance of a magnetic field with the same strength but in a different direction, a multi-orientation multilayered nanofiber assembly could be synthesized, where each layer is made of single-oriented biological nanofibers with the orientation defined by the twisting magnetic field (Figures 1c and 4). Briefly, after the complete drying of the first layer of aligned nanofiber arrays in the presence of a magnetic field, a mixed solution of Fe_3O_4 MNPs and nanofibers were applied onto the first layer and air-dried in a twisted external magnetic field (Figure 1c). Optical microscopy (Figure 4a–c and Figure S6b,d,f) images showed that the nanofiber assemblies were composed of two layers of nanofiber arrays and each layer was made of parallel biological nanofibers, which were aligned in the direction of the external magnetic field applied during the formation of this layer. By using the magnetically guided layer-by-layer deposition method, it is possible to construct large-scale multi-orientation multilayered structures of biological nanofibers with a controlled twisting angle between two neighboring layers, which is dictated by the angle between the magnetic fields applied during the deposition of these two layers. Since the direction of each single layer of biological nanofibers is determined by the applied magnetic field, the final structure of the multi-orientation multilayered nanofiber assemblies can be easily controlled by controlling the applied magnetic field.

Although self-assembled peptide nanotubes[25] and rod-like tobacco mosaic virus (TMV) particles[26] were vertically aligned before by evaporation and interaction between cysteine and metal substrate, respectively, those methods

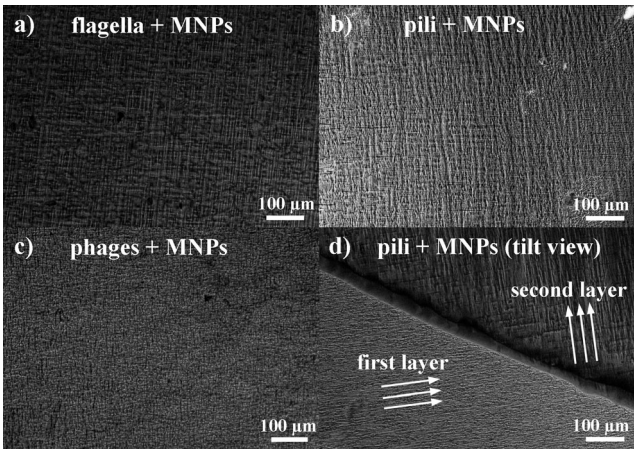

Figure 4. Optical images of double-orientation multilayered nanofiber arrays. a) Optical image of double-orientation layered MNP–flagellum complexes. b) Optical image of double-orientation layered MNP–pilus complexes. c) Optical image of double-orientation layered MNP–phage complexes. d) The tilt view of the peripheral edge (intentionally broken to expose the two layers by removing some materials) of double-orientation layered MNP–pilus complex arrays. Similar views of double-orientation layered flagellum and phage arrays can be found in the Supporting Information (Figure S6).

were limited to rigid peptide nanotubes and TMV, and could not be extended to other biological nanofibers, especially long, flexible (e.g., flagellum), or semiflexible (e.g., M13 phage) biological nanofibers. Moreover, only certain peptides can form nanotubes, and the vertical assembly of TMV relies on the presence of cysteine and the use of a metal substrate, thus those techniques are limited to biomolecules with certain sequences and/or substrates of certain types. Here, we found that biological nanofibers could also be vertically aligned on a substrate by simply allowing the direction of the external magnetic field to be perpendicular to the substrate. Towards this end, Fe_3O_4 MNP solution (70 mg mL^{-1}) was mixed with flagellum solution ($OD_{280nm} = 1.1$) at a volume ratio of 1:100 and air-dried on a cover slide in a constant magnetic field (2 T) with a direction perpendicular to the cover slide (Figure 1 d). SEM imaging (Figure S15) showed that thousands of flagellum–MNP complex nanofibers were standing on the substrate side-by-side along the direction of magnetic field. We did not observe such vertical alignment when either the magnetic field strength or flagellum concentration was reduced (Figure S15 b, c), thus suggesting both a strong magnetic field (2 T) and a high concentration of the nanofiber solution (flagellum concentration, $OD_{280nm} = 1$) are critical to achieve such vertical alignment of biological nanofibers. We also found that the type of substrate does not affect the assembly. The vertical assembly of filamentous hard inorganic nanostructures on a substrate has been used to develop electronic and magnetic devices, biosensors, and medical implants.[27] We envision that the vertical assembly of biological nanofibers could lead to novel structures that can be used to build novel functional devices, given the fact that biological nanofibers can be decorated with functional components such as magnetic, semiconducting, metallic, and bone mineral nanoparticles.[22,28]

Such long-range-ordered nanostructures may be used as unique scaffolds in tissue engineering for controlling the alignment and morphology of resident stem cells, which may in turn direct the proliferation and differentiation of stem cells owing to the unique topography.[27f] In addition, the biological nanofibers we used are all genetically modifiable and can display foreign peptides on the surface by using genetic techniques,[2a,21b,29] thereby providing biochemical cues for directing stem cell behavior. For example, an RGD cell adhesion peptide[30] can be genetically inserted into every subunit of the flagellum using our reported method,[21b] allowing the full display of RGD peptides on the flagellum surface. Displaying RGD peptides on the surface of biological nanofibers can enhance cellular adhesion and growth on them.[31] As a proof of concept, mesenchymal stem cells (MSCs; 1×10^4 cells/mL) were seeded onto the single-orientation parallely aligned arrays (Figure 1 b) of MNP-decorated wild-type flagella (WT-flagellum–MNP) and MNP-decorated RGD-displaying flagella (RGD-flagellum–MNP) and their morphology was monitored. It was found that MSCs did not adhere onto the WT-flagellum–MNP arrays (Figure S16a). However, MSCs were found to adhere onto the RGD-flagellum–MNP arrays (Figure S16b) owing to the display of RGD cell adhesion peptides. More importantly, the MSCs adhered onto the RGD-flagellum–MNP arrays are elongated along the long axis of the flagella. Conversely, MSCs seeded on a control cell culture plate adhered onto the plate but did not show any morphological control (Figure S16c) such as stem cell elongation, which was recently found to favor the stem cell differentiation.[32] These results indicate that our long-range-ordered nanostructures (nanofiber–MNPs) along with tunable surface chemistry (peptide display) are able to direct the fate of stem cells.

In summary, for the first time, we took advantage of the capability of MNPs being aligned along a magnetic field to reproducibly generate large scale assemblies of biological nanofibers with the orientation of the constituent biological nanofibers defined by the applied magnetic field. When decorated with MNPs, the nanofibers could be guided by the external magnetic field to become oriented horizontally (Figure 1 b, c) or vertically (Figure 1 d) with respect to the substrate surface, thereby forming single- and multi-orientation assemblies. We believe that the magnetically directed assembly method is not limited to the three biological nanofibers studied herein, but can be extended to other filamentous supramolecular assemblies for generating long-range-ordered nanostructures. Such long-range-ordered nanostructures can be used as magnetic scaffolds in tissue engineering for promoting the adhesion, proliferation, and differentiation of resident cells.[33] In addition, since the biological nanofibers, such as flagella, pili, and phages, can be biologically engineered to display functional peptides on their surfaces[2a,4b,21b] and decorated with functional nanoparticles,[22,28] an oriented assembly of the peptide-displaying versions of these biological nanofibers is expected to find potential applications in functional devices, materials science, magnetics, electronics, tissue engineering, and nanomedicine.

Experimental Section

Typical alignment experiments: Fe_3O_4 MNPs solution (typically 70 mg mL^{-1}, pH 4.0) was mixed with nanofiber solution (flagellum solution, $OD_{280nm} = 0.1$; pilus solution, $OD_{280nm} = 0.25$; phage solution, 10^{13} pfu mL^{-1}; all biological nanofibers dissolved in water with pH 7.0) and the mixture was allowed to incubate for 10 s at room temperature to form MNP–nanofiber complexes, and then air-dried on a cover slide in a constant magnetic field with a defined direction and strength (Figure 1). Then the dried samples were directly visualized by using a light microscope or coated with a layer of Pt and characterized by using SEM. The magnetic field used here was generated within two parallely placed neodymium cylinder magnets.

Received: May 6, 2013
Published online: September 23, 2013

Keywords: large-scale assemblies · magnetic nanoparticles · magnetic properties · nanostructures

[1] K. F. Jarrell, M. J. McBride, *Nat. Rev. Microbiol.* **2008**, *6*, 466 – 476.
[2] a) B. R. Cao, H. Xu, C. B. Mao, *Angew. Chem.* **2011**, *123*, 6388 – 6392; *Angew. Chem. Int. Ed.* **2011**, *50*, 6264 – 6268; b) E. Hahn, P. Wild, U. Hermanns, P. Sebbel, R. Glockshuber, M. Haner, N. Taschner, P. Burkhard, U. Aebi, S. A. Muller, *J. Mol. Biol.* **2002**, *323*, 845 – 857.
[3] J. W. Kehoe, B. K. Kay, *Chem. Rev.* **2005**, *105*, 4056 – 4072.
[4] a) F. K. Wang, B. R. Cao, C. B. Mao, *Chem. Mater.* **2010**, *22*, 3630 – 3636; b) H. Xu, B. R. Cao, A. George, C. B. Mao, *Biomacromolecules* **2011**, *12*, 2193 – 2199.
[5] C. B. Mao, F. K. Wang, B. R. Cao, *Angew. Chem.* **2012**, *124*, 6517 – 6521; *Angew. Chem. Int. Ed.* **2012**, *51*, 6411 – 6415.
[6] S. W. Lee, C. B. Mao, C. E. Flynn, A. M. Belcher, *Science* **2002**, *296*, 892 – 895.
[7] Y. Lin, E. Balizan, L. A. Lee, Z. W. Niu, Q. Wang, *Angew. Chem.* **2010**, *122*, 880 – 884; *Angew. Chem. Int. Ed.* **2010**, *49*, 868 – 872.
[8] E. Iyyamperumal, S. Y. Wang, L. M. Dai, *ACS Nano* **2012**, *6*, 5259 – 5265.
[9] A. Y. Cao, X. F. Zhang, C. L. Xu, J. Liang, D. H. Wu, X. H. Chen, B. Q. Wei, P. M. Ajayan, *Appl. Phys. Lett.* **2001**, *79*, 1252 – 1254.
[10] O. K. Varghese, M. Paulose, C. A. Grimes, *Nat. Nanotechnol.* **2009**, *4*, 592 – 597.
[11] A. M. Munshi, D. L. Dheeraj, V. T. Fauske, D. C. Kim, A. T. J. van Helvoort, B. O. Fimland, H. Weman, *Nano Lett.* **2012**, *12*, 4570 – 4576.
[12] Z. P. Huang, T. Shimizu, S. Senz, Z. Zhang, X. X. Zhang, W. Lee, N. Geyer, U. Gosele, *Nano Lett.* **2009**, *9*, 2519 – 2525.
[13] E. Lai, W. Kim, P. D. Yang, *Nano Res.* **2008**, *1*, 123 – 128.
[14] M. I. B. Utama, Z. P. Peng, R. Chen, B. Peng, X. L. Xu, Y. J. Dong, L. M. Wong, S. J. Wang, H. D. Sun, Q. H. Xiong, *Nano Lett.* **2011**, *11*, 3051 – 3057.
[15] R. B. Frankel, *Annu. Rev. Biophys. Bio.* **1984**, *13*, 85 – 103.
[16] J. Xie, K. Chen, X. Y. Chen, *Nano Res.* **2009**, *2*, 261 – 278.
[17] A. Ahniyaz, Y. Sakamoto, L. Bergstrom, *Proc. Natl. Acad. Sci. USA* **2007**, *104*, 17570 – 17574.
[18] a) M. D. Lynch, D. L. Patrick, *Nano Lett.* **2002**, *2*, 1197 – 1201; b) S. Kumar, H. Kaur, H. Kaur, I. Kaur, K. Dharamvir, L. M. Bharadwaj, *J. Mater. Sci.* **2012**, *47*, 1489 – 1496.
[19] T. Grigorova, S. Pispas, N. Hadjichristidis, T. Thurn-Albrecht, *Macromolecules* **2005**, *38*, 7430 – 7433.
[20] F. K. Wang, S. L. Nimmo, B. R. Cao, C. B. Mao, *Chem. Sci.* **2012**, *3*, 2639 – 2645.
[21] a) D. Li, X. W. Qu, S. M. C. Newton, P. E. Klebba, C. B. Mao, *J. Mater. Chem.* **2012**, *22*, 15702 – 15709; b) F. Wang, D. Li, C. B. Mao, *Adv. Funct. Mater.* **2009**, *19*, 3355 – 3355.
[22] B. R. Cao, H. Xu, C. B. Mao, *Microsc. Res. Tech. Microsc. Res. Tech* **2011**, *74*, 627 – 635.
[23] R. Massart, *IEEE Trans. Magn.* **1981**, *17*, 1247 – 1248.
[24] H. B. Xia, D. M. Cheng, C. Y. Xiao, H. S. O. Chan, *J. Mater. Chem.* **2005**, *15*, 4161 – 4166.
[25] M. Reches, E. Gazit, *Nat. Nanotechnol.* **2006**, *1*, 195 – 200.
[26] X. L. Chen, K. Gerasopoulos, J. C. Guo, A. Brown, C. S. Wang, R. Ghodssi, J. N. Culver, *ACS Nano* **2010**, *4*, 5366 – 5372.
[27] a) I. Gonzalez-Valls, M. Lira-Cantu, *Energy Environ. Sci.* **2009**, *2*, 19 – 34; b) H. Y. Yu, Y. Sun, N. Singh, G. Q. Lo, D. L. Kwong, *Microelectron. Reliab.* **2012**, *52*, 651 – 661; c) W. H. Han, Y. S. Zhou, Y. Zhang, C. Y. Chen, L. Lin, X. Wang, S. H. Wang, Z. L. Wang, *ACS Nano* **2012**, *6*, 3760 – 3766; d) C. L. Hsu, K. C. Chen, *J. Phys. Chem. C* **2012**, *116*, 9351 – 9355; e) P. Offermans, M. Crego-Calama, S. H. Brongersma, *Sens. Actuators B* **2012**, *161*, 1144 – 1149; f) M. J. Dalby, N. Gadegaard, R. Tare, A. Andar, M. O. Riehle, P. Herzyk, C. D. W. Wilkinson, R. O. C. Oreffo, *Nat. Mater.* **2007**, *6*, 997 – 1003; g) S. Oh, K. S. Brammer, Y. S. J. Li, D. Teng, A. J. Engler, S. Chien, S. Jin, *Proc. Natl. Acad. Sci. USA* **2009**, *106*, 2130 – 2135.
[28] a) B. Cao, C. Mao, *Langmuir* **2007**, *23*, 10701 – 10705; b) C. B. Mao, C. E. Flynn, A. Hayhurst, R. Sweeney, J. F. Qi, G. Georgiou, B. Iverson, A. M. Belcher, *Proc. Natl. Acad. Sci. USA* **2003**, *100*, 6946 – 6951; c) C. B. Mao, D. J. Solis, B. D. Reiss, S. T. Kottmann, R. Y. Sweeney, A. Hayhurst, G. Georgiou, B. Iverson, A. M. Belcher, *Science* **2004**, *303*, 213 – 217.
[29] H. B. Zhu, B. R. Cao, Z. P. Zhen, A. A. Laxmi, D. Li, S. R. Liu, C. B. Mao, *Biomaterials* **2011**, *32*, 4744 – 4752.
[30] M. D. Pierschbacher, E. Ruoslahti, *Nature* **1984**, *309*, 30 – 33.
[31] a) L. A. Lee, Q. L. Nguyen, L. Y. Wu, G. Horyath, R. S. Nelson, Q. Wang, *Biomacromolecules* **2012**, *13*, 422 – 431; b) J. L. Wang, L. Wang, X. Li, C. B. Mao, *Sci. Rep.* **2013**, *3*, 1242; c) J. H. Rong, L. A. Lee, K. Li, B. Harp, C. M. Mello, Z. W. Niu, Q. Wang, *Chem. Commun.* **2008**, 5185 – 5187.
[32] a) S. D. Subramony, B. R. Dargis, M. Castillo, E. U. Azeloglu, M. S. Tracey, A. Su, H. H. Lu, *Biomaterials* **2013**, *34*, 1942 – 1953; b) J. M. Bourget, M. Guillemette, T. Veres, F. A. Auger, L. Germain in *Advances in Biomaterials Science and Biomedical Applications* (Ed.: R. Pignatello), InTech, **2013**, DOI: 10.5772/54142.
[33] a) N. Bock, A. Riminucci, C. Dionigi, A. Russo, A. Tampieri, E. Landi, V. A. Goranov, M. Marcacci, V. Dediu, *Acta Biomater.* **2010**, *6*, 786 – 796; b) X. B. Zeng, H. Hu, L. Q. Xie, F. Lan, W. Jiang, Y. Wu, Z. W. Gu, *Int. J. Nanomed.* **2012**, *7*, 3365 – 3378.